JOURNAL OF GEOPHYSICAL RESEARCH, VOL. 106, NO. D2, PAGES 1583–1593, JANUARY 27, 2001

Relevance of mountain waves for the formation of polar stratospheric clouds over Scandinavia: A 20 year climatology

Andreas Dörnbrack and Martin Leutbecher

Institut für Physik der Atmosphäre, Deutschen Zentrum für Luft- und Raumfahrt Oberpfaffenhofen Wessling, Germany

Abstract. A climatology of meteorological conditions necessary for the existence of polar stratospheric clouds (PSCs) over Scandinavia is presented. The frequency of low enough temperatures for synoptic-scale PSCs is compared with the frequency of additional events when mesoscale PSCs might be induced by the adiabatic cooling in mountain waves. The climatology is based on European Centre for Medium-Range Weather Forecasts analyses of the 20 winter seasons 1979–1980 to 1998–1999 and a simple parameterization of mesoscale stratospheric mountain wave activity. The synoptic-scale formation potential of stratospheric clouds is determined as the fraction of time when the stratospheric minimum temperature is less than the thresholds T_{NAT} (PSC of type I) and T_{frost} (PSC of type II). The potential of additional mesoscale formation is computed by reducing the synoptic-scale temperature on dates when stratospheric mountain wave activity is predicted. This simple approach allows an estimate of the climatological relevance of mountain waves for the existence conditions of PSCs above Scandinavia. In the climatological mean, maximum stratospheric mountain wave activity is found in January, and the maximum seasonal winter average for various levels amounts to 11% of all analysis times (i.e., approximately 3 days per month). Based on the temperature analyses the existence conditions for PSCs of type I are dominated by synoptic-scale processes (maximum 36% of all analysis times are conducive to their existence) whereas the additional mesoscale fraction is less than 6%. Suitable conditions of ice PSCs occur less frequently. It is found that episodes of temperatures low enough for the existence of PSC of type II are controlled by mesoscale temperature anomalies induced by stratospheric mountain waves; on the synoptic scale the stratosphere above Scandinavia is almost always warmer than the threshold T_{frost}.

1. Introduction

Several previous studies have indicated that chemical processing in synoptic-scale polar stratospheric clouds (PSCs) is insufficient to explain observations of active chlorine and ozone loss in the Arctic, and a number of explanations have been proposed [*Lutman et al*., 1997; *Bell et al*., 1996; *Douglass et al*., 1993]. In particular, it is recognized that mesoscale cooling events induced by airflow over mountains can lead to important regions of chlorine activation [*Carslaw et al*., 1998a, 1999]. At least two lines of research are to be distinguished: first, to analyze quantitatively the chemical composition of cold aerosols and PSCs by in situ sensors [*Schreiner et al*., 1999] and, second, to estimate the potential importance of mesoscale PSCs in contributing to large-scale chlorine activation, i.e., the climatological relevance of mesoscale mountain wave cooling for the formation of PSCs and the subsequent ozone loss in the Arctic.

PSCs composed by solid particles are classified into two types. PSCs of type II consist of water ice particles and form at temperatures ~4 K below the ice frost point T_{frost}. They are identical to mother-of-pearl clouds as known from meteorological textbooks [e.g., *Wallace and Hobbs*, 1977, pp. 215 and 235]. PSCs of type Ia exist at higher temperatures and consist of nitric acid trihydrate (NAT), where T_{NAT} denotes the threshold temperature for NAT existence [*Hanson and Mauersberger*, 1988]. Furthermore, there is clear evidence for liquid aerosols in the cold polar stratosphere [e.g., *Peter*, 1997]. These so-called PSCs of type Ib consist of ternary HNO_3-H_2SO_4-H_2O solution droplets and form at temperatures ~3–4 K below T_{NAT} [*Carslaw et al*., 1994].

In the present study, the PSC formation potential, i.e., the fraction of time when the stratospheric temperature falls below the threshold values T_{frost} or T_{NAT}, is determined for Scandinavia. Former studies [*Pawson et al*., 1995, 1999] employed different synoptic-scale data sets of the entire Northern Hemisphere for which the position of the Arctic vortex and the amplitude of planetary waves determine the stratospheric temperature and, thus, the synoptic-scale PSC formation potential. Recent observations and modeling studies give evidence that the formation of PSCs in the Arctic can be triggered by mesoscale meteorological processes leading to stratospheric temperature anomalies, i.e., significant deviations to the synoptic-scale temperature field [*Carslaw et al*., 1998a, b]. In particular, topographically excited gravity waves are able to propagate up to stratospheric levels. Here, the adiabatic cooling of air parcels moving along vertically displaced isentropes controls the frequency and amplitude of mesoscale temperature anomalies and the associated occurrence of mountain wave–induced PSCs. This is the first study that investigates the relevance of

Paper number 2000JD900250.
0148-0227/01/2000JD900250$09.00

these mesoscale stratospheric temperature anomalies for the existence conditions of PSCs on a climatological timescale.

Daily analyses of the European Centre for Medium-Range Weather Forecasts (ECMWF) of the 20 winter seasons 1979–1980 to 1998–1999 provide the synoptic-scale data. The additional mesoscale formation potential is estimated by means of a simple parameterization of stratospheric mountain wave activity suggested by *Dörnbrack et al*. [this issue]. This parameterization classifies the synoptic-scale data in periods with and without significant stratospheric wave activity, but it cannot provide the mountain wave amplitude. The usefulness of this simple parameterization of mountain wave activity has been evaluated by comparing it to mesoscale temperature anomalies computed with a nonlinear numerical model for a one-month integration over Scandinavia.

The whole procedure consists of three steps: (1) determination of periods of stratospheric wave activity in the synoptic-scale analyses, (2) calculation of the synoptic-scale PSC formation potential, and (3) estimation of the additional mesoscale PSC formation potential by subtracting an assumed mountain wave amplitude from the synoptic-scale minimum temperature on dates of stratospheric wave activity. The last step implies horizontal mountain wavelengths smaller than or comparable to the domain size of the considered region. Under this assumption, mesoscale stratospheric cooling and warming of air parcels along vertically displaced streamlines occurs certainly above the mountain ridge. However, for the present study only cooling effects in mountain waves are of importance as they constitute conditions where PSCs may form and chlorine species become finally activated.

Section 2 reports on the frequency of stratospheric mountain wave activity. The synoptic-scale and mesoscale PSC formation potential is presented in section 3. After a discussion in section 4 the paper is concluded in section 5.

2. Mountain Wave Activity

A 20-winter record (1979–1980 till 1998–1999) of daily (0000, 0600, 1200, and 1800 UT) ECMWF analyses serves as input to investigate the mountain wave activity and the climatological relevance of stratospheric mountain wave cooling above Scandinavia. The data are analyzed in two distinct geographical regions (Plate 1). They are called "Kebnekaise" and "Glittertind" according to the highest peaks in each area. We only use data of the winter months December, January, February, and March because in this period the stratospheric temperatures are low enough to support the formation of polar stratospheric clouds.

The data set consists of two parts. ECMWF Reanalysis (ERA) data [*Gibson et al*., 1997] cover the first 14 winters, 1979–1980 until 1992–1993. The spectral T106 data are evaluated on a regular grid of $1.125° \times 1.125°$ resolution in latitude and longitude and on 15 standard pressure levels between 1000 and 10 hPa. The remaining 6 winters are taken from the operational ECMWF analyses truncated at T106 and evaluated on the same standard pressure levels.

Dörnbrack et al. [this issue] propose simple dynamical criteria to classify the synoptic-scale flow into periods of large and small mountain wave activity in the stratosphere. Periods of significant mountain wave activity are diagnosed when the low-level wind is strong V_H (900 hPa) $> V_*$ (criterion C1) and nearly perpendicular to the mountains $300° - \Delta\alpha_* < \alpha_H < 300° + \Delta\alpha_*$ (criterion C2), where 300° is approximately normal to the orientation of the Scandinavian mountain range. In order to exclude wave absorption at critical levels the directional shear between the wind direction at 900 hPa and all the levels 500, 300, 100, and 50 hPa must be less than $\Delta\alpha_*$ (criterion C3). For January 1997, periods of stratospheric wave activity identified in this fashion are compared to results of a one-month mesoscale simulation [*Dörnbrack et al*., this issue]. These periods are found to be strongly correlated with simulated mesoscale stratospheric temperature anomalies induced by mountain waves. It should be noted that the above simple parameterization of wave activity does not take into account processes controlling the wave amplitude in the stratosphere, e.g., those due to change of thermal stability at the tropopause. It only describes whether stratospheric mountain waves are likely or not.

Averaged values of V_H and α_H are calculated on isobaric surfaces from the ECMWF analyses over all grid points for each region Kebnekaise and Glittertind (The control areas Kebnekaise and Glittertind consist of 36 and 77 analysis grid points, respectively). Then, the above criteria are checked at each analysis time t_a which is representative for a 6 hour period $t_a \pm 3$ hours. When all the conditions C1, C2, and C3 are satisfied simultaneously, periods of significant mountain wave activity are identified separately for each control area. The frequency of mountain wave activity depends on the threshold values for wind speed and direction (V_* and $\Delta\alpha_*$). In order to study the sensitivity of this simple parameterization, two different thresholds (V_*; $\Delta\alpha_*$) equal to (10 m/s; 45°) and (12 m/s; 30°) are compared.

In Figures 1 and 2 the resulting periods of significant mountain wave activity are plotted for all days in the 20 winter seasons 1979–1980 till 1998–1999 (bar code, see Figure 1 for Kebnekaise and Figure 2 for Glittertind). The bar code reveals periods of mountain wave activity ranging from one single analysis time to a couple of consecutive days. On the basis of the bar code, the monthly frequency of stratospheric mountain wave activity is computed (Figure 3). Generally, there is a strong interannual variability in the time series of winter months without apparent trend or dominating period of oscillation. Winters of high mountain wave activity occur simultaneously in both regions (e.g., 1988–1989 until 1992–1993 and 1996–1997); however, the respective frequencies differ. On the basis of the 20-winter-seasons data set the mean monthly frequency of mountain wave activity is computed (Table 1). The frequency of mountain wave activity peaks in January and is lowest in March in both geographical regions. The large standard deviations represent the significant interannual variations of the parameterized stratospheric gravity wave activity.

The climatological seasonal frequencies (December–March) of stratospheric mountain wave activity for values (V_*; $\Delta\alpha_*$) = (10 m/s; 45°) are 11.4% of all analysis times (i.e., approximately 3 days) per month in Kebnekaise and 14.2% for Glittertind. The frequency of mountain wave activity is reduced by roughly 60% if we apply the more strict criterion of (12 m/s; 30°) to the synoptic-scale analyses. This means that the frequency is quite sensitive to the threshold values for wind speed V_* and direction $\Delta\alpha_*$.

In the companion paper, *Dörnbrack et al*. [this issue] show for January 1997 and the control area Kebnekaise that the periods where mountain wave–induced stratospheric temperature anomalies exceeding 2 K exist are well correlated with the periods where the three criteria C1, C2, and C3 are satisfied simultaneously. Thus we propose that the climatological

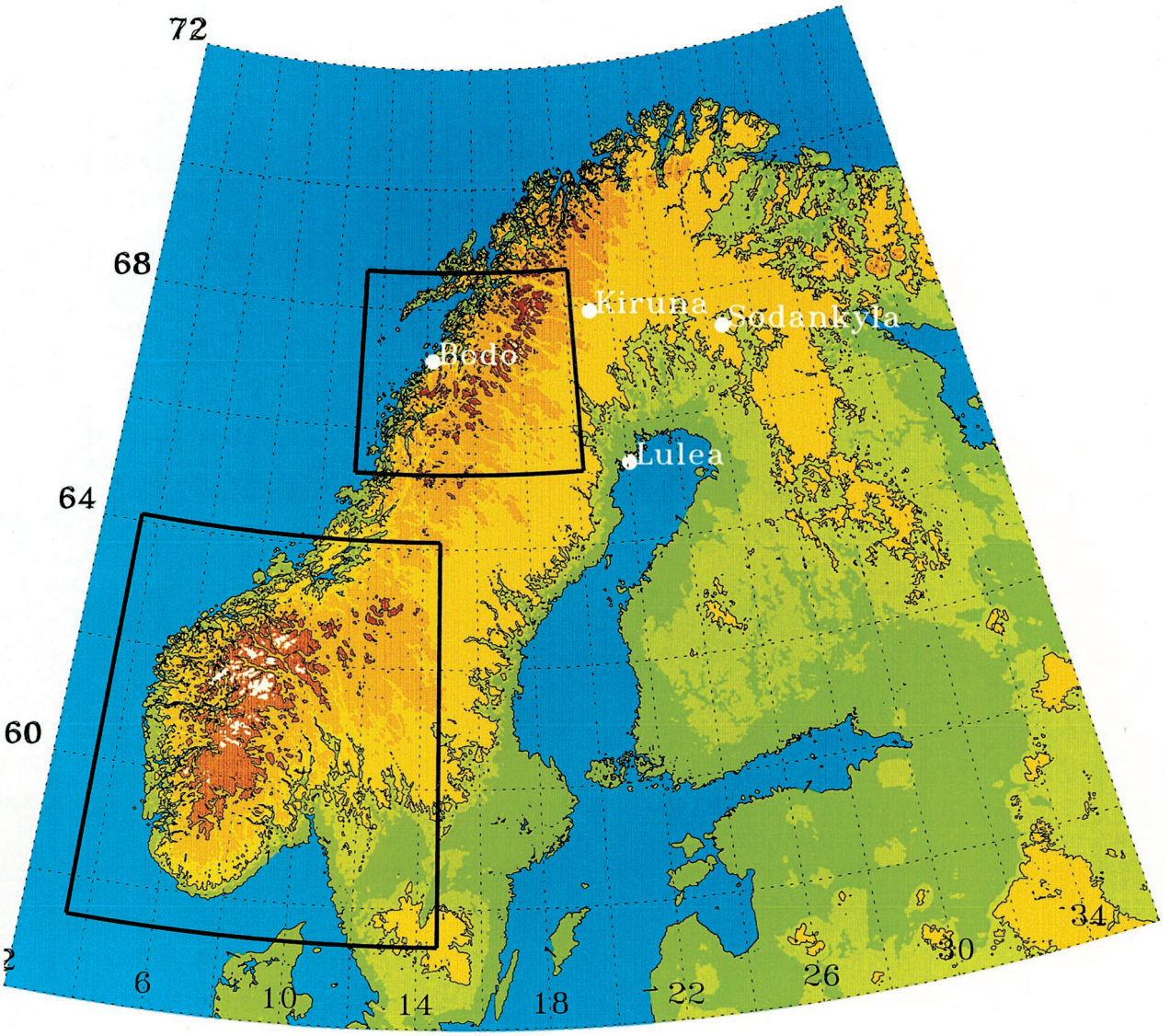

Plate 1. Map of Scandinavia control regions "Kebnekaise" (north) and "Glittertind" (south). Color code of terrain heights: 1–100 m, green; 100–200 m, yellow; 200–500 m, light brown; 500–1000 m, brown; 1000–2000 m, dark brown; and above 2000 m, white. Contour lines are at 1, 200, and 1000 m, respectively.

frequency of significant stratospheric mountain wave activity according to C1, C2, and C3 is an upper bound to the frequency where mountain waves may trigger the formation of additional PSCs. The actual frequency will be lower as, additionally, it is required that the synoptic-scale temperature be within a certain range. This is examined in section 3.

3. Climatology of PSC Formation Potential

Synoptic-scale minimum temperatures $T_{\min}$ are determined on isobaric surfaces p equals 70, 50, and 30 hPa at each analysis time t_a in the two control regions. We define the formation potential of synoptic-scale PSCs of type I (type II) at a pressure level p in the control area A as the (dimensionless) frequency

$$v_s = m_s/N,$$

where N is the number of analysis times in the considered period (e.g., 31×4 for a December month with time interval between consecutive analyses of $\Delta t = 6$ hours) and m_s is the number of analysis times where the minimum temperature of the analyses in the control area A at pressure p is less than T_{NAT} (type I) or T_{frost} (type II) (mixing ratios of 5 ppmv and 10 ppbv for H_2O and HNO_3, respectively, are used for the calculation of the existence temperatures T_{frost} and T_{NAT} following *Hanson and Mauersberger* [1988]). Thus the dimensionless frequencies v_s can be interpreted as the time fraction where the temperature is below the respective threshold values. We will consider monthly frequencies, seasonal frequencies (December–March) and their climatological averages.

The formation potential of additional mesoscale PSCs of type I (type II) is

$$v_{m+} = m_{m+}/N,$$

where N is as above and m_{m+} is the number of analyses where (1) there is significant stratospheric mountain wave activity expected according to C1, C2, and C3 (see Figures 2 and 3) and (2) the minimum temperature of the analyses in the control area A at pressure p is less than $T_{\mathrm{NAT}} + \Delta T$ (type I) or $T_{\mathrm{frost}} +$

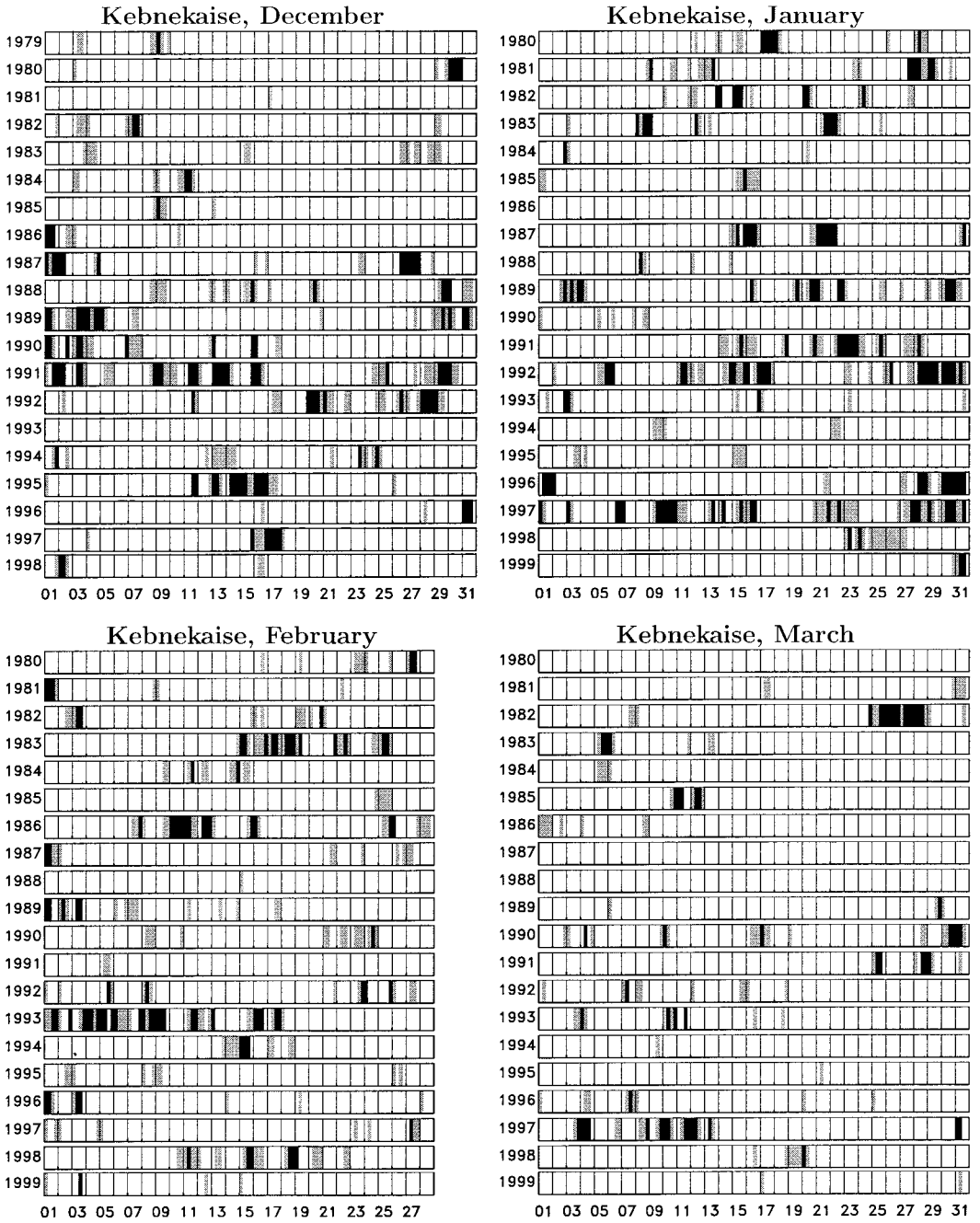

Figure 1. Classification indicating periods of significant mountain wave activity in the stratosphere ("bar code") for the control area Kebnekaise in December, January, February, and March during the winter seasons 1979–1980 until 1998–1999. The threshold values (V_*; $\Delta\alpha_*$) are (10 m s^{-1}; 45°) (grey) and (12 m s^{-1}; 30°) (black).

ΔT (type II) and larger than T_{NAT} (type I) or T_{frost} (type II). Then $v = v_s + v_{m+}$ is the total formation potential.

Dörnbrack et al. [this issue] have shown that periods of predicted wave activity are strongly correlated with mesoscale stratospheric temperature anomalies ΔT exceeding 2 K and up to 8 K with respect to synoptic-scale values. Because the parameterization presented in section 2 does not provide the magnitude of adiabatic cooling in each wave, we set ΔT equal to 4 and 8 K. These values represent hydrostatic mountain waves of horizontal wavelengths smaller than the domain size of the control regions and with a medium peak-to-peak amplitude of ~400 and 800 m, respectively. Extreme mountain waves with amplitudes greater than 12 K, as simulated, e.g., by *Leutbecher and Volkert* [1996], are rare and exceptional events and will therefore not be considered in this climatological study.

The calculation of the formation potential based on the frequencies v_s and v_{m+} results in an upper bound for the actual formation of PSCs in the respective region. In most of the events the mountain wave amplitude is less than 8 K. Furthermore, the parameterization does not consider the limited spatial extent of stratospheric clouds. It is likely that only

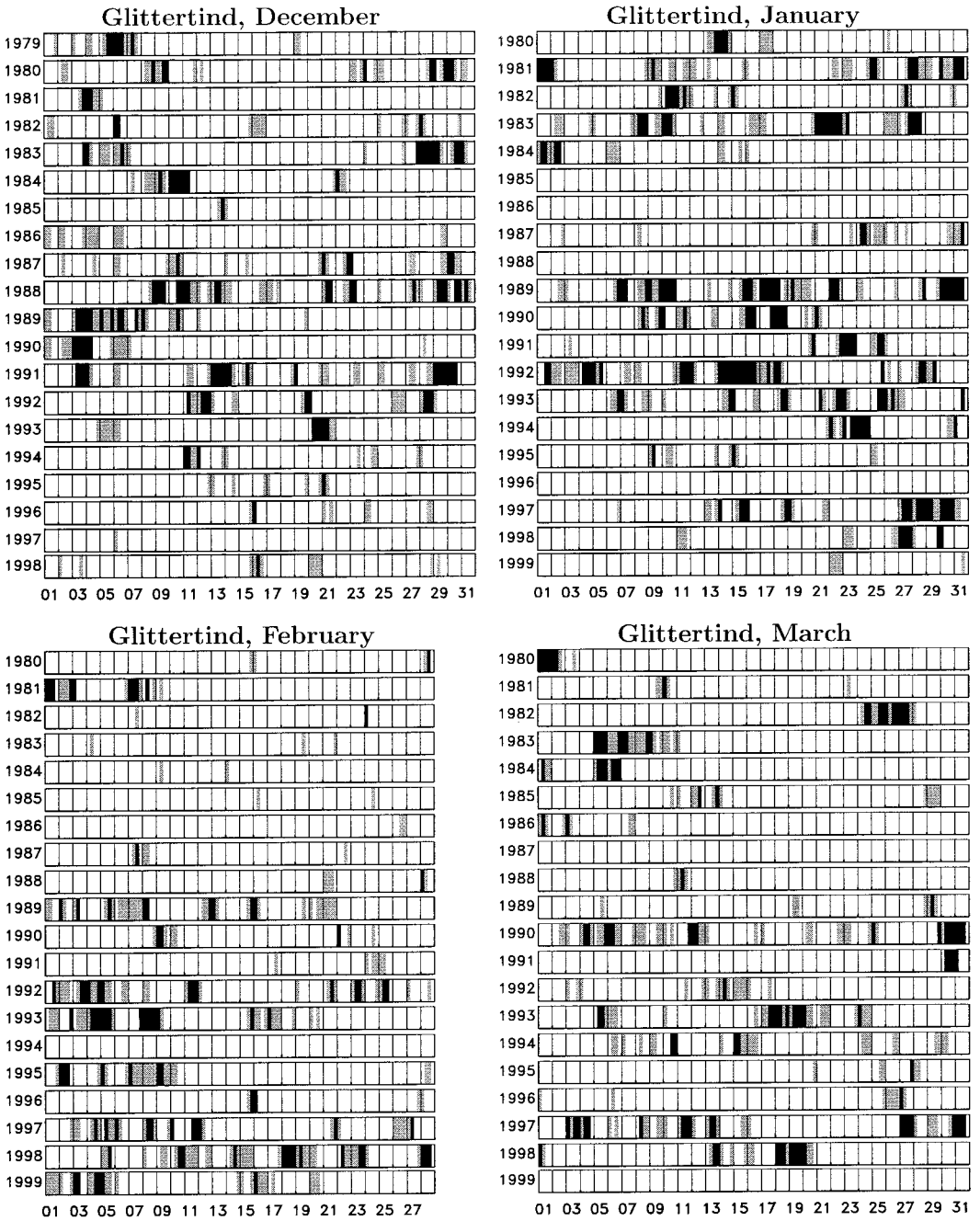

Figure 2. Classification indicating periods of significant mountain wave activity in the stratosphere (bar code) for the control area Glittertind in December, January, February, and March during the winter seasons 1979–1980 until 1998–1999. The threshold values (V_*; $\Delta\alpha_*$) are (10 m s^{-1}; 45°) (grey) and (12 m s^{-1}; 30°) (black).

a small fraction of the control area A is covered by mountain wave–induced PSCs. The uncertainty of the assumed mixing ratios of H_2O and HNO_3 influences the values of T_{NAT} and T_{frost} and, consequently, the frequencies v_s and V_{m+}. Whereas the former two processes reduce the formation potential, the sign of the latter effect is largely unknown. The influence of the accuracy of the synoptic-scale analyses will be discussed in section 4.

Figure 4 shows v_s and v_{m+} of type I PSCs for the winter seasons (December–March) from 1979–1980 to 1998–1999 for the control area Kebnekaise. Here, $V_* = 10$ m/s, $\Delta\alpha_* = 45°$, and $\Delta T = 8$ K are used. Generally, the fraction of time when only mountain wave activity brings the temperature below T_{NAT} is small compared to the fraction of time when synoptic temperatures are below T_{NAT}. The monthly frequency v_s oscillates between 0% (synoptic-scale PSCs of type I are very unlikely) and a maximum value of 95% (at 30 hPa in January 1996). In most winters, mesoscale mountain waves contribute only marginally (V_{m+} is generally less than 10%) although maximum values of 25% (January 1997) have been determined. The monthly climatological averages of v_s and v_{m+} for PSC type I existence conditions are summarized in Table 2 for

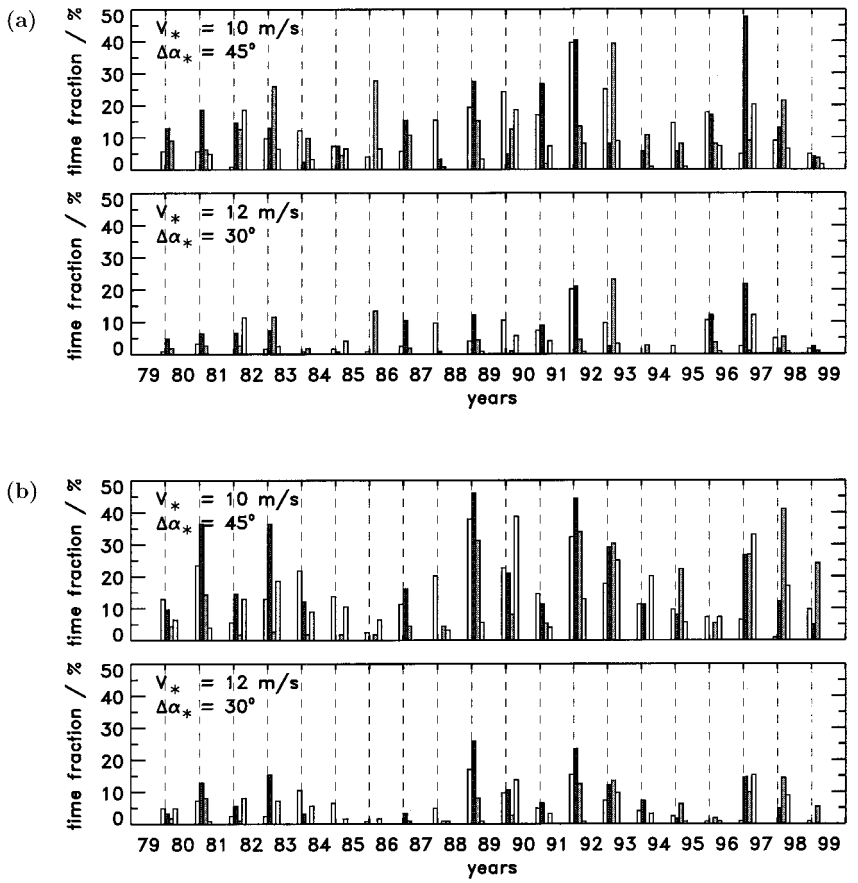

Figure 3. Average monthly stratospheric mountain wave activity in percent of time for the winter months December, January, February, and March (white, black, grey, and white, respectively) above control areas (a) Kebnekaise and (b) Glittertind from 1979–1980 until 1998–1999. A time fraction of 10% is equivalent to a period of approximately 3 days per month. The threshold values (V_*; $\Delta\alpha_*$) of (10 m s^{-1}; 45°) and (12 m s^{-1}; 30°) are plotted for each area.

all winter months. According to these values the total formation potential v is maximum in January. In January and February, when the Arctic vortex is usually stable and cold, the synoptic-scale contributions v_s are 4–7 times larger than the respective mesoscale portions v_{m+}. In December and March, however, when the polar stratosphere is warmer and in transition from or to the summer circulation regime, mesoscale processes become more important and can reach the magnitude of the synoptic-scale values.

The picture is quite different if we consider PSCs of type II in the northern control area Kebnekaise (Figure 5 and Table 2). First, their formation potentials v_s and v_{m+} are much smaller than those of PSCs of type I. Second, mesoscale contributions dominate the total PSC type II formation potential; that is, v_{m+} for PSCs of type II is in almost all investigated winter months larger than that of synoptic-scale PSCs. As for PSCs of type I, most favorable conditions for ice cloud formation occur in January and February when the synoptic-scale temperatures are low and close to the thresholds T_{NAT} and T_{frost} (see Table 2).

Because of warmer stratospheric temperatures in the southern control area Glittertind, the synoptic-scale PSC type I formation potential v_s is smaller than in Kebnekaise (Table 3). On the other hand, the predicted mountain wave activity (see Table 1) is slightly higher, and mesoscale effects are expected to become more important. Indeed, the values of additional mesoscale effects are larger than for the northern control area (with only one exception: December PSC of type I at 50 hPa). Furthermore, the ratio of synoptic-scale to mesoscale formation potential is smaller and ranges from 0.7 to 3.8 (instead of

Table 1. Mean Monthly Frequency of Stratospheric Wave Activity in Percent for Two Threshold Values (V_*; $\Delta\alpha_*$) of the Simple Parameterization in Section 2

Month	10 m s^{-1}; 45°	12 m s^{-1}; 30°
	Kebnekaise	
December	12.1 ± 9.5	4.7 ± 5.0
January	14.4 ± 12.3	6.0 ± 6.5
February	12.5 ± 9.3	4.1 ± 5.6
March	6.5 ± 6.0	2.3 ± 3.5
Average	11.4	4.3
	Glittertind	
December	14.7 ± 9.2	5.1 ± 4.8
January	16.9 ± 14.4	7.5 ± 7.5
February	13.3 ± 13.0	4.3 ± 4.9
March	12.0 ± 10.3	4.4 ± 4.5
Average	14.2	5.3

The monthly averages and standard deviations are calculated over the 20 winter seasons 1979–1980 till 1998–1999 for the control areas "Kebnekaise" and "Glittertind." The last row for each control area denotes the seasonal average.

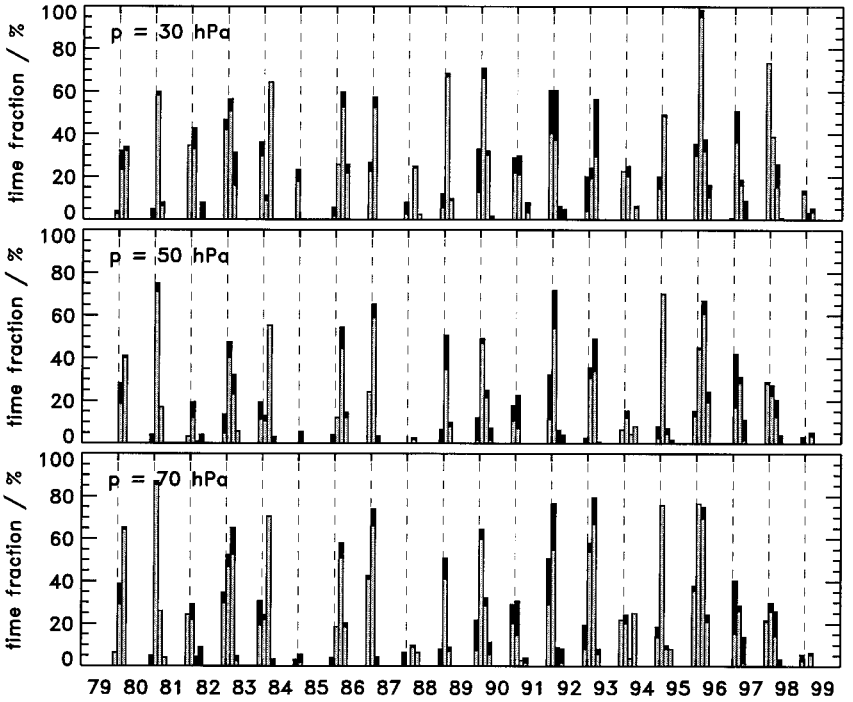

Figure 4. Total formation potential of PSCs of type I at 30, 50 and 70 hPa for the winter months December, January, February, and March above Kebnekaise. Grey bars, frequency v_s of synoptic-scale PSCs; black tops, additional mesoscale PSC formation potential v_{m+}, where the threshold values for the mountain wave activity are $(V_*; \Delta\alpha_*) = (10 \text{ m s}^{-1}; 45°)$ and the wave amplitude is assumed to be $\Delta T = 8$ K. The threshold values T_{NAT} are 192, 195, and 198 K for the above pressure levels, respectively.

4 to 7 for Kebnedaise), i.e., even for PSCs of type I, mesoscale processes can be equally important as the synoptic-scale cooling, at least in certain periods (especially in December and March). The results of Table 3 reveal fewer PSCs of type II for all months, and again, mountain wave–induced PSCs dominate the results.

The mesoscale PSC formation potential v_{m+} is reduced by a factor of 2–2.5 at all levels in both regions if a lower temperature amplitude $\Delta T = 4$ K is considered. Note that the results presented in this section are based on the less strict mountain wave activity criterion of $V_* = 10$ m/s and $\Delta\alpha_* = 45°$. Employing the stricter thresholds of $V_* = 12$ m/s and $\Delta\alpha_* = 30°$ results in an additional 60% reduction of mesoscale activity and, hence, in a further decrease of suitable conditions for the formation of mountain wave–induced PSCs.

4. Discussion

The formation potentials v_s and v_{m+} characterize necessary conditions for the existence of PSCs in terms of a temperature-dependent on/off switch depending on the threshold values T_{NAT} and T_{frost}. Whether PSCs are actually formed in the considered region depends also on the actual mixing ratios of water vapor and nitric acid trihydrate, on the stratospheric aerosol content, and on the history of air parcels passing the Scandinavian mountain range. In situ observations of solid

Table 2. Mean Formation Potential of PSCs in Control Area Kebnekaise

	70 hPa		50 hPa		30 hPa	
Month	Synoptic-Scale	Mesoscale	Synoptic-Scale	Mesoscale	Synoptic-Scale	Mesoscale
			Type I PSCs			
December	14.0 ± 13.0	5.6 ± 5.6	5.8 ± 8.1	4.2 ± 5.1	19.5 ± 18.1	6.0 ± 5.9
January	36.5 ± 26.2	6.4 ± 7.0	28.1 ± 22.5	6.7 ± 6.7	35.1 ± 24.6	5.2 ± 5.6
February	25.3 ± 26.1	4.0 ± 4.2	18.0 ± 16.3	3.7 ± 4.1	16.6 ± 18.4	4.2 ± 6.6
March	5.1 ± 7.4	2.6 ± 3.3	2.5 ± 5.0	2.0 ± 2.6	2.2 ± 5.2	2.0 ± 2.9
			Type II PSCs			
December	0.0 ± 0.0	1.9 ± 3.9	0.0 ± 0.0	1.0 ± 3.5	0.2 ± 0.7	3.5 ± 4.7
January	1.4 ± 2.5	7.1 ± 7.2	1.3 ± 2.6	5.9 ± 6.4	2.7 ± 3.8	7.3 ± 7.8
February	2.5 ± 4.4	4.6 ± 6.9	0.4 ± 1.0	4.6 ± 6.4	1.8 ± 3.8	4.1 ± 5.2
March	0.0 ± 0.0	0.4 ± 1.2	0.0 ± 0.0	0.5 ± 1.3	0.0 ± 0.0	0.2 ± 0.7

PSCs of type I, i.e., periods when $T_{\text{min}} < T_{\text{NAT}}$ (synoptic-scale) and $T_{\text{min}} < T_{\text{NAT}} + \Delta T$ (mesoscale), and PSCs of type II, i.e., periods when $T_{\text{min}} < T_{\text{frost}}$ (synoptic-scale) and $T_{\text{min}} < T_{\text{frost}} + \Delta T$ (mesoscale), where $\Delta T = 8$ K, are shown. Values are in percent of time for each month. The mountain wave activity is estimated by the criterion $V_* = 10$ m s^{-1} and $\Delta\alpha_* = 45°$ (bar code in Figure 1). The minimum temperature is estimated on surfaces of constant pressure, and the climatological average is over the 20 winter seasons 1979–1980 till 1998–1999.

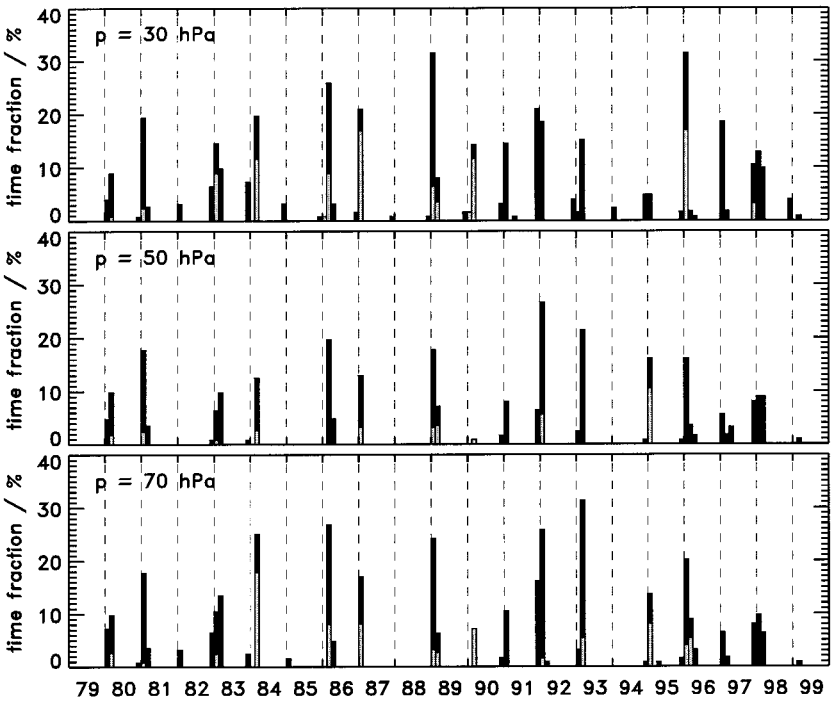

Figure 5. Total formation potential of PSCs of type II at 30, 50, and 70 hPa for the winter months December, January, February, and March above Kebnekaise. Grey bars, frequency v_s of synoptic-scale PSCs; black tops, additional mesoscale PSC formation potential v_{m+}, where the threshold values for the mountain wave activity are $(V_*; \Delta\alpha_*) = (10 \text{ m s}^{-1}; 45°)$ and the wave amplitude is assumed to be $\Delta T = 8$ K. The threshold values T_{frost} are 185, 188, and 191 K for the above pressure levels, respectively.

PSCs of type I in the Arctic have shown that these clouds spent several days in air with temperature close to or below T_{NAT} [*Larsen et al.*, 1997]. Alternatively, large-amplitude temperature fluctuations as in mountain waves can push the temperature below T_{frost} and support the nucleation to solid particles on much shorter timescales [*Meilinger et al.*, 1995; *Carslaw et al.*, 1999]. In this study, we do not consider microphysical details of PSC formation. The temperature-dependent switch between PSC and no PSC constitutes the starting point of the present climatology. Thus the computed magnitude of the PSC formation potential depends on the accuracy of ECMWF temperature analyses for the synoptic-scale frequencies v_s and, additionally, on the parameters V_*, $\Delta\alpha_*$, and ΔT for the mesoscale frequencies v_{m+}.

The T106 L31 (31 model levels from the surface to 10 hPa) ECMWF analyses constitute a unique data set for estimating the relevance of mountain wave cooling on the formation potential of PSCs over Scandinavia for the past 20 winter seasons 1979–1980 till 1998–1999. Our climatology is restricted to stratospheric levels (70, 50, and 30 hPa) well below the top of the ECMWF model at 10 hPa where the temperature analyses are mostly erroneous. The deviations between observations and analyses at these levels are generally less than 1 K as reported by *Uppala* [1997, p. 109, Figure 55]. There, the zonally

Table 3. Mean Formation Potential of PSCs in Control Area Glittertind

	70 hPa		50 hPa		30 hPa	
Month	Synoptic-Scale	Mesoscale	Synoptic-Scale	Mesoscale	Synoptic-Scale	Mesoscale
			Type I PSCs			
December	7.5 ± 8.1	6.1 ± 4.9	3.2 ± 4.4	3.7 ± 4.3	12.3 ± 16.1	7.2 ± 5.2
January	22.3 ± 19.6	7.8 ± 7.7	16.2 ± 17.9	8.0 ± 6.9	26.2 ± 21.5	7.5 ± 6.8
February	17.6 ± 21.9	4.6 ± 6.6	12.7 ± 15.5	3.8 ± 5.4	15.1 ± 17.1	4.9 ± 6.9
March	3.8 ± 5.8	3.5 ± 3.7	2.1 ± 4.6	2.5 ± 3.0	1.8 ± 4.9	2.5 ± 3.0
			Type II PSCs			
December	0.0 ± 0.2	0.9 ± 3.0	0.0 ± 0.0	0.4 ± 1.3	0.0 ± 0.0	2.1 ± 4.5
January	0.3 ± 0.8	6.1 ± 7.1	0.2 ± 0.7	4.6 ± 6.7	2.0 ± 3.7	7.0 ± 8.7
February	0.5 ± 1.0	2.1 ± 4.0	0.2 ± 0.6	1.6 ± 2.8	1.3 ± 2.3	2.3 ± 4.3
March	0.0 ± 0.0	0.5 ± 1.4	0.0 ± 0.0	0.4 ± 1.1	0.0 ± 0.0	0.3 ± 0.7

PSCs of type I, i.e., periods when $T_{\text{min}} < T_{\text{NAT}}$ (synoptic-scale) and $T_{\text{min}} < T_{\text{NAT}} + \Delta T$ (mesoscale), and PSCs of type II, i.e., periods when $T_{\text{min}} < T_{\text{frost}}$ (synoptic-scale) and $T_{\text{min}} < T_{\text{frost}} + \Delta T$ (mesoscale), where $\Delta T = 8$ K, are shown. Values are in percent of time for each month. The mountain wave activity is estimated by the criterion $V_* = 10 \text{ m s}^{-1}$ and $\Delta\alpha_* = 45°$ (bar code in Figure 2). The minimum temperature is estimated on surfaces of constant pressure, and the climatological average is over the 20 winter seasons 1979–1980 till 1998–1999.

averaged bias of the stratospheric temperature reanalyses for polar regions (60°–90°N) is maximum in the layer from 30 to 20 hPa and amounts to ~0.2–0.4 K. Below this layer (from 50 to 30 hPa and from 70 to 50 hPa) the absolute value of the bias is less than 0.2 K.

The recent refinement of the analysis scheme and higher horizontal and vertical resolutions of the current ECMWF model have improved the quality of stratospheric temperature analyses. An inspection of T213 L31 model analyses (horizontal grid resolution ≈60 km) on selected days of January 1997 actually shows signatures of mountain waves in the temperature distributions above northern Scandinavia. However, neither the temperature amplitude ΔT nor the vertical structure of these waves are sufficiently resolved to attain a mountain wave cooling similar to that found in observations and mesoscale model simulations with horizontal grid resolutions of ~4 km during the same period [*Wirth et al*., 1999]. At present, one possible way for studying the climatological relevance of mountain wave–induced PSCs is to use the long-term T106 ECMWF analyses plus a simple parameterization of stratospheric mountain wave activity.

Because of only few direct observations of stratospheric mountain wave cooling, its frequency of occurrence and the vertical excursions of streamlines during such events can be either determined by linear wave theory or by nonlinear numerical simulations of airflow over mountains. *Carslaw et al*. [1999], on the basis of a linear mountain wave forecast model [*Bacmeister et al*., 1994], use ΔT ranging from 12 to 19 K to calculate the NAT production due to mountain waves. Such large amplitudes require vertical displacements of isentropic surfaces of more than 1200 m. For typical vertical wavenumbers $m = N_b/U = 0.02\ \mathrm{s}^{-1}/20\ \mathrm{m\ s}^{-1} \approx 1\ \mathrm{km}^{-1}$ the product of m and the vertical displacement is on the order of unity, and therefore wave overturning and breaking are expected [*Shutts et al*., 1988]; N_b and U are the upstream stratospheric buoyancy frequency and wind speed, respectively. These events are very seldom because of turbulent breakdown usually limiting the amplitude growth of the gravity waves at stratospheric levels. This process cannot be treated realistically in the linear wave model, and frequently, the temperature decrease is overpredicted. Here, we use a simple parameterization of mountain wave activity, the bar code developed by *Dörnbrack et al*. [this issue].

The third parameter in the parameterization is the amplitude ΔT of the cooling due to the adiabatic ascent in stratospheric mountain waves. Thus the temperature minimum in the presence of significant mountain wave activity is assumed to be lower than the synoptic-scale temperature minimum by ΔT at most. Mesoscale simulations reveal that periods of predicted wave activity are strongly correlated with stratospheric temperature anomalies of up to $\Delta T \approx 8$ K with respect to synoptic-scale conditions [*Dörnbrack et al*., this issue]. Therefore values of ΔT equal to 4 and 8 K as assumed in this study represent nonbreaking hydrostatic mountain waves of horizontal wavelength larger than 150 km (~10 times the horizontal grid length; see discussion of *Leutbecher and Volker* [2000]) and with amplitudes between 400 and 800 m [*Shutts et al*., 1988].

On the basis of these parameters the synoptic-scale and mesoscale formation potential of PSCs was determined in both control regions. Our synoptic-scale PSC I formation potential of 35% for January at 30 hPa (see Table 2) agrees well with results of *Pawson et al*. [1995]. They found that at least one point in the Northern Hemisphere was colder than T_{NAT} on 34% of all days in a winter season in a 18 year record. The close agreement can be explained because in a climatological mean the coldest stratospheric region is found in an area encompassing the North Pole and centered between 20° and 80°E, i.e., close to Scandinavia and our control area Kebnekaise. In agreement with that study we find a maximum frequency of suitable conditions for PSC type I formation in January.

It is well known that the synoptic-scale dynamics of the stratospheric polar vortex is mainly influenced by the propagation and breakdown of planetary waves [e.g., *Baldwin and Dunkerton*, 1998]. On some occasions the formation of PSCs of type II might be influenced by the adiabatic ascent in amplifying planetary waves as concluded by *Pawson et al*. [1995] and *Teitelbaum and Sadourny* [1998]. In addition to these large-scale processes we found vertically propagating mesoscale mountain waves controlling the total formation potential for PSC of type II above Scandinavia.

This result corresponds to visual observations of mother-of-pearl clouds in northern Scandinavia that go back to *Mohn* [1893] and *Störmer* [1931, 1934]. They found a considerable correlation between the appearance of mother-of-pearl clouds and a Föhn-like weather situation with strong tropospheric winds from west-northwest, i.e., nearly perpendicular to the mountain range. These observations confirm our first two parameterization criteria for mountain wave activity. *Dietrichs* [1950] analyzed systematically a total of 96 reported PSC observations from the period 1889–1949 and concluded that in more than 75% of the cases their occurrence was associated with deep surface lows traveling above the Norwegian Sea toward the northeast leading to strong tropospheric winds. Recent observations by *Enell et al*. [1999] at Kiruna indicate a larger number of PSC events of type II than predicted by synoptic-scale temperature data due to the frequent presence of stratospheric mountain waves.

Similarly to *Pawson et al*. [1995], we found a considerable interannual variability of the total PSC formation potential v as well as of the synoptic-scale flow regimes during the 20 winter seasons 1979–1980 till 1998–1999. It is beyond the scope of the present paper to discuss every winter in detail. Meteorological overviews of the individual northern hemispheric winters are given by *Naujokat and Labitzke* [1993], *Pawson et al*. [1995], *Naujokat and Pawson* [1996], *Hansen and Hoppe* [1997], and *Coy et al*. [1997]. However, it should be mentioned that the total formation potential v is small in years with sudden stratospheric warmings (1980–1981, 1984–1985, 1985–1986, 1988–1989, 1991–1992, and 1998–1999). In these winters the increase of stratospheric temperatures occurred either as Canadian-type warming early in December or as minor or major warmings in January or February. In the long-lasting period without major warming from 1991 till 1998 the values of v are generally larger.

Our study is restricted to regions directly above the Scandinavian mountains. This means that only effects of vertically propagating hydrostatic gravity waves have been taken into account. Longer waves are influenced by the Coriolis force and produce further mesoscale temperature anomalies downstream of the mountain range. These are not considered although they increase the amount of air affected by mountain wave cooling. Generally, the issue of the spatial extent of mesoscale temperature anomalies in the stratosphere is not covered here but requires attention in future investigations.

Starting in 1991–1992, field campaigns were regularly undertaken in northern hemispheric winters to observe PSCs in

Scandinavia. Unfortunately, no comprehensive overview of date and location, altitude, and type of all the observed PSCs exists. Thus only some particular observations (mostly under clear-sky conditions) are available for a comparison. However, these comparisons must be restricted to some singular case studies and cannot be expanded to climatological timescales.

5. Summarizing Conclusions

A 20 year data set of 6-hourly ECMWF analyses has been employed to calculate the formation potential of PSCs of types I and II above Scandinavia. Its synoptic-scale fraction v_s is determined as the frequency of all analysis dates when the stratospheric minimum temperature is less than the thresholds T_{NAT} and T_{frost}. The additional mesoscale formation potential v_{m+} is computed by simple dynamical criteria of stratospheric wave activity. The synoptic-scale wind speed and direction in relation to the parameters V_* and $\Delta\alpha_*$ determine periods of significant stratospheric wave activity. Physically, these criteria are based on long-term radiosonde observations and on results of linear wave theory, and they are verified with nonlinear mesoscale numerical simulations for numereous case studies. In our approach, another parameter, the temperature amplitude ΔT, controls the mesoscale mountain wave cooling. To our knowledge, the present study is the first estimate of the climatological relevance of mesoscale mountain wave cooling on the existence conditions of polar stratospheric clouds above Scandinavia.

Maximum stratospheric mountain wave activity is found in January. The seasonal winter average is 11.4% for $V_* = 10$ m s^{-1} and $\Delta\alpha_* = 45°$, and this value is reduced by 60% if stricter criteria are applied (12 m s^{-1} and 30°). Synoptic-scale conditions dominate the total formation potential v of PSCs of type I in contrast to the marginal mesoscale fraction: A maximum frequency v_s of 36.5% at 70 hPa (28.1% at 50 and 35.1% at 30 hPa) exists in January whereas mesoscale processes additionally contribute maximum 6.6%. The PSC type II formation potential is dominated by orographically induced gravity waves. Altogether, the formation potentials of PSCs of type II are much smaller than those of PSCs of type I. The mesoscale contribution v_{m+} reaches maxima 7.1 and 7.3% in January at 70 and 30 hPa, respectively. For this PSC type the synoptic-scale fraction v_s of 1.4 and 2.7% is small. Although the stratosphere is generally warmer above the southern control area Glittertind compared to Kebnekaise, mesoscale mountain wave–induced PSCs of type I become equally frequent as synoptic-scale PSCs in December and March.

The present study does not aim at providing a quantitative parameterization of the temperature anomalies induced by mountain waves; our aim is rather to estimate the influence of mountain waves on the total PSC formation potential $v = v_s + v_{m+}$ above a specific region. Further efforts with respect to a quantitative parameterization in the entire Northern Hemisphere and estimates of the induced ozone depletion are still needed and require careful comparisons with observations as well as with mesoscale simulation results. Detailed information on cooling rates and the amplitudes in mountain wave events are also required to design and validate parameterizations of mountain wave cooling for use in global models. A validation of the presented formation potential of PSCs as a whole is hardly possible. However, both the parameterization of mountain waves as well as the representation of the PSC microphysics can be improved. Each of these components of the presented climatology can be verified against observations independently. This remains a task for future studies.

Acknowledgments. This work was supported by the BMBF in the framework of the German Ozone Research Programme. The data were kindly provided by Klaus-Peter Hoinka, principal investigator of the ECMWF special project "The Climatology of the Tropopause." Agathe Untch (ECMWF Reading) is acknowledged for providing T213 L31 analyses.

References

Bacmeister, J. T., P. A. Newman, B. L. Gary, and K. R. Chan, An algorithm for forecasting mountain wave-related turbulence in the stratosphere, *Weather Forecasting*, *9*, 241–253, 1994.

Baldwin, M. P., and T. J. Dunkerton, Biennial, quasi-biennial, and decadal oscillations of potential vorticity in the Northern Hemisphere, *J. Geophys. Res*., *103*, 3919–3928, 1998.

Bell, W., C. Paton-Walsh, T. D. Gardiner, P. T. Woods, N. R. Swann, N. A. Martin, L. Donohoe, and M. P. Chipperfield, Measurements of stratospheric chlorine monoxide (ClO) from ground-based FTIR observations, *J. Atmos. Chem*., *24*, 285–297, 1996.

Carslaw, K. S., B. P. Luo, S. Clegg, T. Peter, P. Brimblecombe, and P. Crutzen, Stratospheric aerosol growth and HNO_3 gas phase depletion from coupled HNO_3 and water uptake by liquid particles, *Geophys. Res. Lett*., *21*, 2479–2482, 1994.

Carslaw, K. S., et al., Increased stratospheric ozone depletion due to mountain-induced atmospheric waves, *Nature*, *391*, 675–678, 1998a.

Carslaw, K. S., M. Wirth, A. Tsias, B. P. Luo, A. Dörnbrack, M. Leutbecher, H. Volkert, W. Renger, J. T. Bacmeister, and T. Peter, Particle microphysics and chemistry in remotely observed mountain polar stratospheric clouds, *J. Geophys. Res*., *103*, 5785–5796, 1998b.

Carslaw, K. S., T. Peter, J. T. Bacmeister, and S. D. Eckerman, Widespread solid particle formation by mountain waves in the Arctic stratosphere, *J. Geophys. Res*., *104*, 1827–1836, 1999.

Coy, L., E. R. Nash, and P. A. Newman, Meteorology of the polar vortex: Spring 1997, *Geophys. Res. Lett*., *24*, 2693–2696, 1997.

Dietrichs, H., Über die Entstehung der Perlmutterwolken, *Meteorol. Rundsch*., *3*, 208–213, 1950.

Dörnbrack, A., M. Leutbecher, J. Reichardt, A. Behrendt, K. -P. Müller, and G. Baumgarten, Relevance of mountain wave cooling for the formation of polar stratospheric clouds over Scandinavia: Mesoscale dynamics and observations for January 1997, *J. Geophys. Res*., this issue.

Douglass, A., R. Rood, J. Waters, L. Froidevaux, W. Read, L. Elson, M. Geller, Y. Chi, M. Cerniglia, and S. Steenrod, A three-dimensional simulation of the early winter distribution of reactive chlorine in the north polar vortex, *Geophys. Res. Lett*., *20*, 1271–1274, 1993.

Enell, C.-F., Å. Steen, T. Wagner, U. Frieß, K. Pfeilsticker, U. Platt, and K. -H. Fricke, Occurrence of polar stratospheric clouds at Kiruna, *Ann. Geophys*., *17*, 1457–1462, 1999.

Gibson, R., P. Kållberg, S. Uppala, A. Hernandez, A. Nomura, and E. Serrano, ERA description, *ECMWF Re-Anal. Proj. Rep. Ser. 1*, 72 pp., Eur. Cent. for Medium-Range Weather Forecasts, Shinfield Park, Reading, Berkshire, England, U.K., 1997.

Hansen, G., and U. -P. Hoppe, Lidar observations of polar stratospheric clouds and stratospheric temperature in winter 1995/96 over northern Norway, *Geophys. Res. Lett*., *24*, 131–134, 1997.

Hanson, D., and K. Mauersberger, Laboratory studies of the nitric acid trihydrate: Implications for the south polar stratosphere, *Geophys. Res. Lett*., *15*, 855–858, 1988.

Larsen, N., B. M. Knudsen, J. M. Rosen, N. T. Kjome, R. Neuber, and E. Kyrö, Temperature histories in liquid and solid polar stratospheric cloud formation, *J. Geophys. Res*., *102*, 23,505–23,517, 1997.

Leutbecher, M., and H. Volkert, Stratospheric temperature anomalies and mountain waves: A three-dimensional simulation using a multiscale weather prediction model, *Geophys. Res. Lett*., *23*, 3329–3332, 1996.

Leutbecher, M., and H. Volkert, The propagation of mountain waves into the stratosphere: Quantitative evaluation of three-dimensional simulations, *J. Atmos. Sci*., *57*, 3090–3108, 2000.

Lutman, E. R., J. A. Pyle, M. P. Chipperfield, D. J. Lary, I. Kilbane-Dawe, J. W. Waters, and N. Larsen, Three-dimensional studies of

the 1991/92 Northern Hemisphere winter using domain-filling trajectories with chemistry, *J. Geophys. Res*., *102*, 1479–1488, 1997.
Meilinger, S. K., T. Koop, B. P. Luo, T. Huthwelker, K. S. Carslaw, P. J. Crutzen, and T. Peter, Size-dependent stratospheric droplet composition in lee wave temperature fluctuations and their potential role in PSC freezing, *Geophys. Res. Lett*., *22*, 3031–3034, 1995.
Mohn, H., Irisierende Wolken, *Meteorol. Z*., *10*, 81–97, 1893.
Naujokat, B., and K. Labitzke, Collection of reports on the stratospheric circulation during the winters 1974/75–1991/92, *Rep. 1*, 301 pp., Sol. Terr. Energy Program (STEP), Sci. Comm. on Sol.-Terr. Phys., Int. Counc. of Sci. Unions, Paris, France, 1993.
Naujokat, B., and S. Pawson, The cold stratospheric winters 1994/95 and 1995/96, *Geophys. Res. Lett*., *23*, 3703–3706, 1996.
Pawson, S., B. Naujokat, and K. Labitzke, On the polar stratospheric cloud formation potential of the northern stratosphere, *J. Geophys. Res*., *100*, 23,215–23,225, 1995.
Pawson, S., K. Krüger, R. Swinbank, M. Bailey, and A. O'Neill, Intercomparison of two independent stratospheric analyses: Temperatures relevant to polar stratospheric cloud formation, *J. Geophys. Res*., *104*, 2041–2050, 1999.
Peter, T., Microphysics and heterogeneous chemistry of polar stratospheric clouds, *Annu. Rev. Phys. Chem*., *48*, 785–822, 1997.
Schreiner, J., C. Voigt, A. Kohlmann, F. Arnold, K. Mauersberger, and N. Larsen, Chemical analysis of polar stratospheric cloud particles, *Science*, *283*, 968–970, 1999.
Shutts, G. J., M. Kitchen, and P. H. Hoare, A large amplitude gravity wave in the lower stratosphere detected by radiosonde, *Q. J. R. Meteorol. Soc*., *114*, 579–594, 1988.
Störmer, C., Höhe und Farbverteilung der Perlmutterwolken, *Geofys. Publ*., *IX*, 3–25, 1931.
Störmer, C., Höhenmessungen von Stratosphärenwolken, *Beitr. Phys. Atmos*., *21*, 1–6, 1934.
Teitelbaum, H., and R. Sadourny, The role of planetary waves in the formation of polar stratospheric clouds, *Tellus Ser. A*, *50*, 302–312, 1998.
Uppala, S., Observing system performance in ERA, ECMWF *Re-Anal. Proj. Rep. Ser. 3*, Eur. Cent. for Medium-Range Weather Forecasts, Shinfield Park, Reading, Berkshire, England, U. K., 1997.
Wallace, J. M., and P. V. Hobbs, *Atmospheric Science: An Introductory Survey*, 467 pp., Academic, San Diego, Calif., 1977.
Wirth, M., A. Tsias, A. Dörnbrack, V. Weiß, K. S. Carslaw, M. Leutbecher, W. Renger, H. Volkert, and T. Peter, Model guided Lagrangian observation and simulation of mountain polar stratospheric clouds, *J. Geophys. Res*., *104*, 23,971–23,981, 1999.

A. Dörnbrack and M. Leutbecher, Institut für Physik der Atmosphäre, DLR Oberpfaffenhofen, D-82230 Wessling, Germany. (andreas.doernbrack@dlr.de)

(Received July 20, 1999; revised March 13, 2000;
accepted March 13, 2000.)